CHEMICAL ENGINEERING TRANSACTIONS Volume 24, 2011
Editor Sauro Pierucci

 ISBN 978-88-95608-15-0 ISSN 1974-9791
DOI: 10.3303/CET1124232

Vortex Shape in Unbaffled Stirred Vessels: Experimental Study v*ia* Digital Image Analysis

Antonio Busciglio, Franco Grisafi, Francesca Scargiali, Maria Luisa Davì, Alberto Brucato

Università degli Studi di Palermo
Dipartimento di Ingegneria Chimica dei Processi e dei Materiali
Viale delle Scienze, ed. 6, 90128, Palermo, Italy

There is a growing interest in using unbaffled stirred tanks for addressing certain processing needs. In this work, digital image analysis coupled with a suitable shadowgraphy-based technique is used to investigate the shape of the free-surface vortex that forms in uncovered unbaffled stirred tanks.
The technique is based on back-lighting the vessel and suitably averaging vortex shape over time. Impeller clearance from vessel bottom and tank filling level are varied to investigate their influence on vortex shape. A correlation is finally proposed to fully describe vortex shape also when the vortex encompasses the impeller.

1. Introduction

The main feature of unbaffled stirred tanks is the highly tangential liquid motion, that leads to the formation of a central vortex on the liquid free surface. Free-surface vortexing is often undesirable, but may be useful in several cases (Smit and During, 1991; Ciofalo et al., 1996; Haque et al. 2006).
First vortex modeling attempt is due to Nagata (1975), who considered the vessel contents as subdivided in two parts: the *forced vortex zone* (nearby the shaft, characterized by rigid motion, i.e. constant angular velocity) and the *free vortex zone* (characterized by constant angular momentum).
Smit and During. (1991) found that actual radial gradients of tangential velocity are smaller than in Nagatas's model and suggested relevant modifications. They also confirmed that vortex depth linearly depends on Froude number, though with a proportionality coefficient somewhat different than in Nagata's findings. Several further works dealt with measurement or review of vortex scale-up criteria (Markopoulos et al. 1995; Rao et al. 2009). More recently, a few works addressed the set up of suitable CFD models for free-surface unbaffled tanks (Ciofalo et al., 1996; Cartland Glover and Fitzpatrick, 2007; Lamarque et al. 2010), so confirming the growing interest towards this type of apparatus.

2. Experimental set-up

The experimental system here investigated was an uncovered unbaffled cylindrical vessel (diameter $T = 0.19\ m$) with a flat base equipped with Rushton turbine ($D = T/3$).

Please cite this article as: Busciglio A., Grisafi F., Scargiali F., Davi M.L. and Brucato A., 2011, Vortex shape in unbaffled stirred vessels: experimental study via digital image analysis, Chemical Engineering Transactions, 24, 1387-1392
DOI: 10.3303/CET1124232

The liquid phase was deionized water. System geometry was varied by changing liquid rest height (from $H_0 = 0.75T$ to $H_0 = 1.25T$) as well as impeller clearance from vessel bottom (from $C = T/6$ to $C = T/2$). For each investigated case, several impeller velocities in the range *100-1000 rpm* were used.
The gas-liquid system was back-illuminated by two lamps shielded by a *5mm* Nylon sheet as a light diffuser. The vessel was immersed in a square tank filled with water in order to minimize optical distortions. For each experiment, 100 images were collected by means of a MVblueFOX C2514-M CCD camera operated at 5 frames per second.

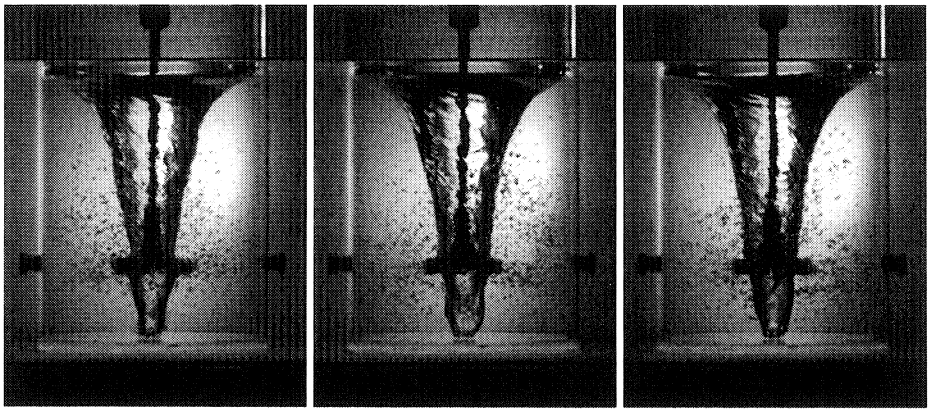

Figure 1: Typical snapshots of the system ($C = T/3$, $H_0 = T$, $N = 800rpm$).

In Fig.1 a typical snapshot sequence is reported for one of the investigated systems. The back-lighting technique clearly allows a good observation of vortex shape. Notably, the vortex is far from being smooth, since rippling is present, due to the small instabilities of liquid surface and eruption of small bubbles ingested by the vortex itself.
The imaging technique here adopted is based on pixelwise averaging of luminance values $L(x,y)$ over an acquisition time sufficiently long in order to obtain a smooth averaged image:

$$\bar{L}(x,y) = \frac{1}{N}\sum_{i=1}^{N} L(x,y) \tag{1}$$

In the present case, a number if images equal to $N = 100$ was always found to result into sufficiently stable average images. In Fig.2a-b, typical averaged images are shown. It is possible to observe that at the lowest agitation speed the vortex is highly defined, but becomes more blurred while increasing impeller speed. At the highest speed some noise into the liquid bulk can also be observed, due to the presence of bubbles generated by the interaction between the vortex and the impeller. To investigate these phenomena, the pixelwise image variance was computed, as:

$$\bar{V}(x,y) = \frac{1}{N}\sum_{i=1}^{N}\left[L(x,y) - \bar{L}(x,y)\right]^2 \tag{2}$$

The variance image so computed allows visual observation of the moving parts in the image itself, i.e. allows to easily observe the average amplitude of instantaneous vortex fluctuations and/or vortex rippling, as it can be observed in Fig.2 c-d.

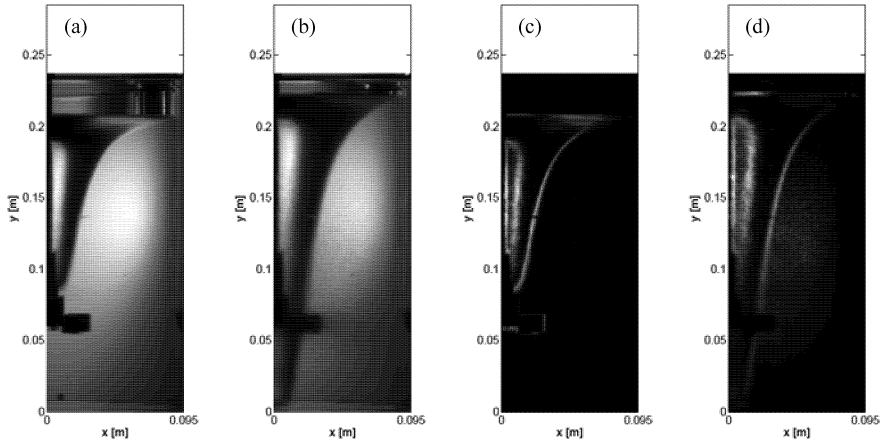

Figure 2:Typical averaged images of standard geometry vessel (C = T/3, H_0 = T): 500rpm (a) and 900rpm (b), and relevant variance images (c,d).

3. Vortex characterization

Once the time averaged image of the vessel has been obtained, it is possible to fit a suitable curve for describing vortex shape. In this contribution, the well accepted vortex shape description based on the *critical radius* r_c formerly proposed by Nagata (1975) was preliminarily adopted.

$$r_c = \frac{T}{2}\sqrt{\frac{T}{2} - \sqrt{\left(\frac{T}{2}\right)^2 - \frac{2g(H_w - H_b)}{\Omega^2}}} \tag{3}$$

$$z = \begin{cases} H_b + \dfrac{\Omega^2 r_c^2}{2g}\left(2 - \dfrac{r_c^2}{r^2}\right) \rightarrow \text{Free Vortex Region} \\ H_b + \dfrac{\Omega^2}{2g} r^2 \rightarrow \text{Forced Vortex Region} \end{cases} \tag{4}$$

Where Ω is the impeller angular velocity (*rad/s*) and g is the gravitational acceleration. As it can be seen, the only parameters needed are the maximum liquid height at vessel lateral wall H_w and the vortex bottom height H_b (notably, if the liquid volume is known, only the difference H_w-H_b is needed to describe vortex profile, as the other parameter can in principle be obtained)

A first qualitative analysis of images pointed out some basic facts: i) the Nagata model fails to describe vortex shape (dashed lines in Fig.3); (ii) if an effective "shape preserving" H_{sp} is substituted for H_b, by suitably adjusting its value this modified Nagata model results in a thorough description of the outer portion of the vortex, but obviously completely misses the inner vortex shape; iii) Nagata's model fails to describe vortex shape when vortex bottom falls below the impeller.

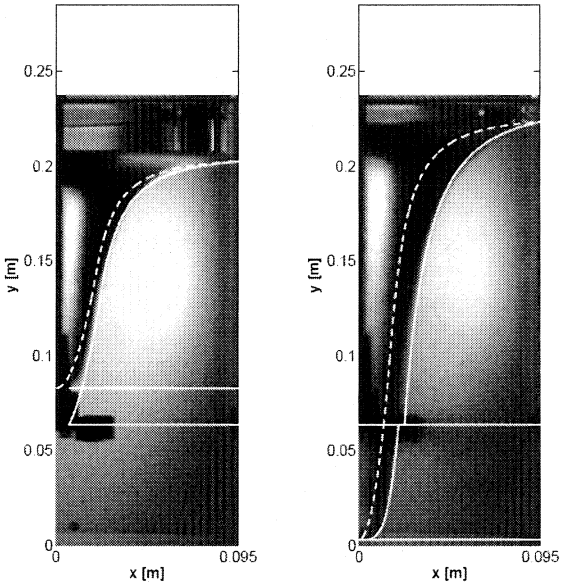

Figure 3:Typical time averaged images of standard geometry vessel equipped with Rushton turbine and relevant fitting with the proposed model (C = T/3, H_0 = T, N = 500rpm, 800rpm).

On this basis, the present experimental campaign was aimed at measuring the values H_w, H_{sp}, H_b for different cases and at developing a suitable correlation for vortex shape prediction. The H_w and H_b were directly measured from images, while H_{sp} was obtained by fitting the modified Nagata model equations (Eqns. 3-4 with H_{sp} substituted for H_b) with H_{sp} acting as the only outer vortex shape parameter. During experiments, the rotational speed at which vortex bottom reaches the impeller plane (hereafter referred to as the *critical speed,* N_{cr}) was also assessed for all vessel configurations.
By introducing the *critical Froude number* N_{cr}^2D/g in conjunction with the common Froude number (N^2D/g), the following novel equation is proposed for the description of the inner vortex when vortex bottom falls below the impeller (*supercritical* conditions):

$$z\big|_{r\le r_c} = H_b + \left(\frac{12g}{\Omega}\right)^4 \frac{r^4}{r_c^3} \quad ; \quad (Fr > Fr_{cr}) \tag{5}$$

As it can be seen in Fig.3, where typical sub- and over-critical systems are shown, the modified Nagata model here proposed (solid lines) works very well at all Froude numbers.

For each experimental condition, from the averaged vortex images the relevant values of H_w, H_{sp} and H_b were assessed. These are reported in Fig.4 (left) versus Froude number. It can be seen that, as a difference from H_b, H_{sp} can become significantly negative, with only a small trend change when impeller speed exceeds the critical value.

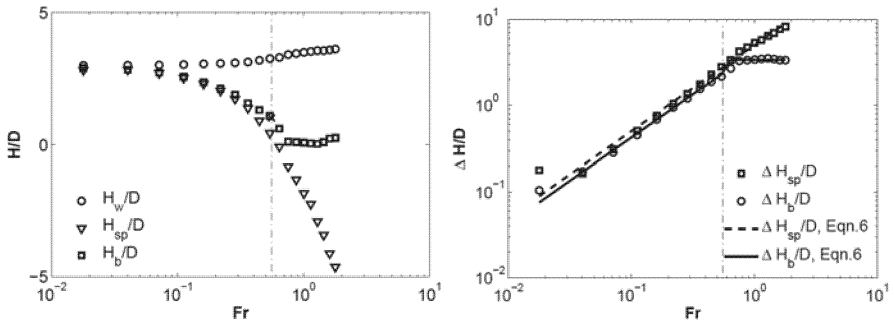

Figure 4: Vortex parameters (left) and relevant dimensionless shape depths as a function of the Froude number (Rushton turbine, C = T/3, H_0 = T). Dot-dashed lines highlight the Fr_{cr} value.

Similarly to the Nagata model, if the liquid volume is known only the values $\Delta H_{sp} = (H_w - H_{sp})$ and $\Delta H_b = (H_w - H_b)$ are really needed to fully describe vortex shape. In Fig.4 (right) all ΔH_{sp} and ΔH_b obtained with $C=T/3$ and $H_0=T$, are reported *versus* Froude number. Notably, for $Fr<Fr_{cr}$ linear trends are obtained, in agreement with previous literature findings (Markopoulos and Kontogeorgaki, 1995). This consideration applies very well to both ΔH_{sp} and ΔH_b, with the latter always slightly smaller than the former.
For $Fr>Fr_{cr}$,the ΔH_b attains an almost constant value, as the actual vortex-bottom height cannot fall below vessel bottom. Conversely, the ΔH_{sp} values continue to follow a linear trend. No comparison with previous findings is possible in this case, as to the authors knowledge no information exists for $Fr>Fr_{cr}$ in the scientific literature. On the basis of the observed trends, the following expressions are proposed to describe the vortex depth curves:

$$\frac{\Delta H_{sp}}{D} = k_{sp} Fr\,; \qquad \frac{\Delta H_b}{D} = \begin{cases} k_b Fr & \rightarrow Fr \le Fr_{cr} \\ k_{b,cr} & \rightarrow Fr > Fr_{cr} \end{cases} \tag{6}$$

In Fig.5 (left), the Critical Froude number observed for different vessel geometrical configurations is reported. Notably, a linear increase of Fr_{cr} is observed with vessel shape factor. In Fig.5 (right), the parameters needed for using Eqn.6 are reported as a function of the vessel shape factor and compared with literature data (Markopulos and Kontogeorgaki, 1995). As it can be seen, the results obtained for sub-critical systems are very close to those obtained for ΔH_b by Markopulos and Kontogeorgaki (1995); notably no distinction between ΔH_{sp} and ΔH_b was made by these authors.
As concerns the super-critical regimes, the same ΔH_{sp} curve describes vortex depth regardless of the regime, while the ΔH_b curve is different from that pertaining to the subcritical regime. Clearly, by Eqns 3,4,5 and 6 and the information reported in Fig.5 the vortex shape for unbaffled uncovered tanks with various liquid fillings and impeller

clearances can be thoroughly assessed for supercritical regimes. For subcritical regimes the outer vortex portion (notably the most important for vessel properties assessment) is also thoroughly described, while as concerns the inner vortex, the H_b values may be deduced while work is under way to provide a suitable model equation.

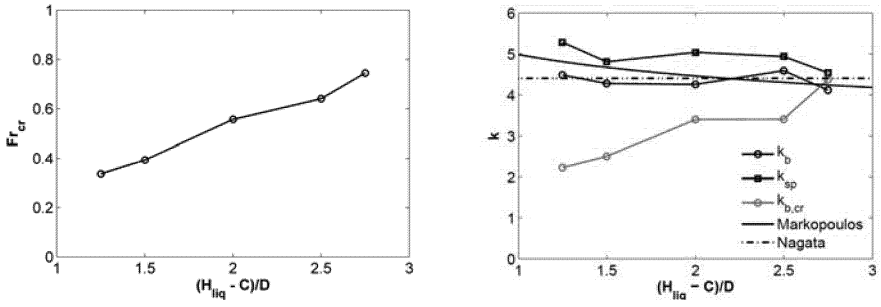

Figure 5: Critical Froude number (left) and dimensionless shape depths as a function of a vessel shape factor (Rushton turbine, C = T/3, H_0 = T).

4. Conclusions

In this work, a simple image analysis technique was adopted to measure vortex shape in unbaffled stirred tanks equipped with a Rushton turbine for various clearances of the turbine and tank filling levels. A novel correlation was proposed that better describes vortex shape and also extends above Fr_{cr} .

References

Cartland Glover G.M., Fitzpatrick J.J., 2007, Modelling vortex formation in an unbaffled stirred tank reactors, Chem Eng. J., 127, 11-12

Ciofalo M., Brucato A., Grisafi F., Torraca N., 1996, Turbulent flow in closed and free-surface unbaffled tanks stirred by radial impellers, Chem. Eng. Sci., 51(14), 3557-3573

Haque J.N., Mahmud T., Roberts K.J., Rhodes D., 2006, Modeling turbulent flows with free-surface in unbaffled agitated vessel, Ind. Eng Chem. Res., 45, 2881-2891.

Lamarque N., Zoppè B., Lebaigue O., Dolias Y., Bertrand M., Ducros F., 2010, Large eddy simulation of the turbulent free-surface flow in an unbaffled stirred tank reactor, Chem. Eng. Sci., 65, 4307-4322.

Markopoulos J., Kontogeorgaki E., 1995, Vortex depth in unbaffled single and multiple impeller agitated vessels, Chem. Eng. Technol., 18, 68-74.

Nagata S., 1975, Mixing: principles and applications, Wiley, New York.

Rao A.R., Kumar B. Patel A.K., 2009, Vortex behaviour in an unbaffled surface aerator, Science Asia, 35, 183-188.

Smit L., During J., 1991, Vortex geometry in stirred vessel, In: Proceedings of the 7th European Congress of Mixing, vol.2, Bruges, Belgium, 633-639.